Supporting Information

# Sonochemical Synthesis of Zr-based metal-organic cages and their adsorption performance towards Tartrazine

De-Sheng Wei,[a] Jian Li,[a] Ting-Ting Xu,[a] Wan-Yi Lan,[a] Nan Lv,[a]

Yu-Teng Zhang*[a] and Shuang-Bao Li*[b]

[a] *College of Chemical Engineering, Northeast Electric Power University, Jilin City 132012, PR China. E-mail: zhangyuteng@neepu.edu.cn (Y.-T. Zhang).*
[b] *School of Chemical and Pharmaceutical Engineering, Jilin Institute of Chemical Technology, Jilin, 132022, PR China. E-mail: lishuangbao@jlict.edu.cn (S.-B. Li)*
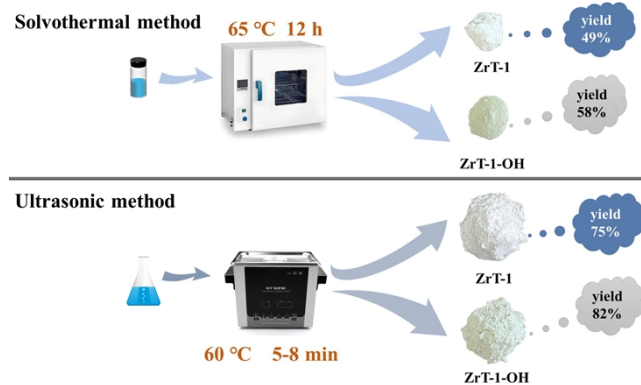
**Fig.S1** Comparison of the preparation process for Zr-MOCs based on sonochemical method and traditional solvothermal method.
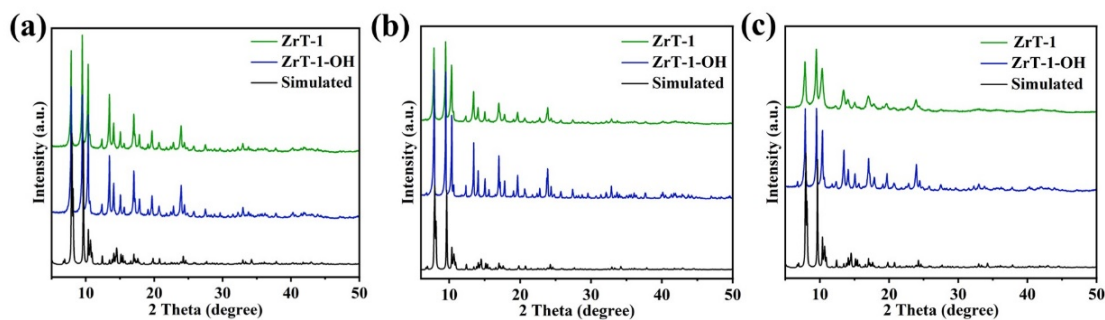


**Fig.S2** PXRD under varying synthesis conditions: (a) 150 W, 30 ℃, 40 kHz; (b) 75 W, 60 ℃, 40 kHz; (c) 75 W, 30 ℃, 40 kHz.
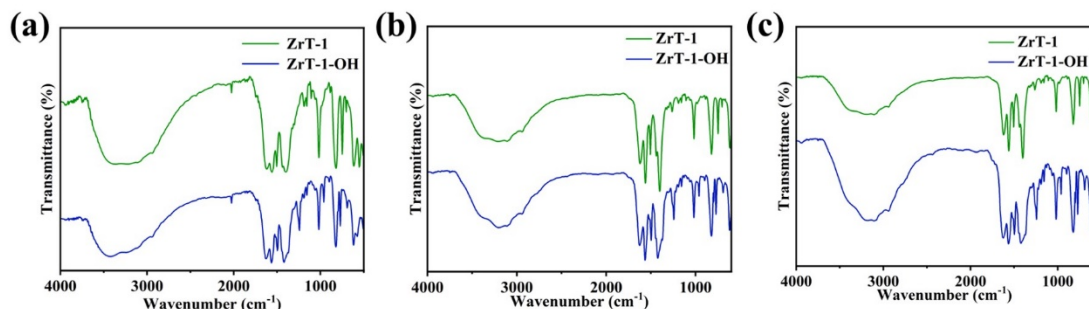


**Fig.S3** FT-IR under varying synthesis conditions: (a) 150 W, 30 ℃, 40 kHz; (b) 75 W, 60 ℃, 40 kHz; (c) 75 W, 30 ℃, 40 kHz.
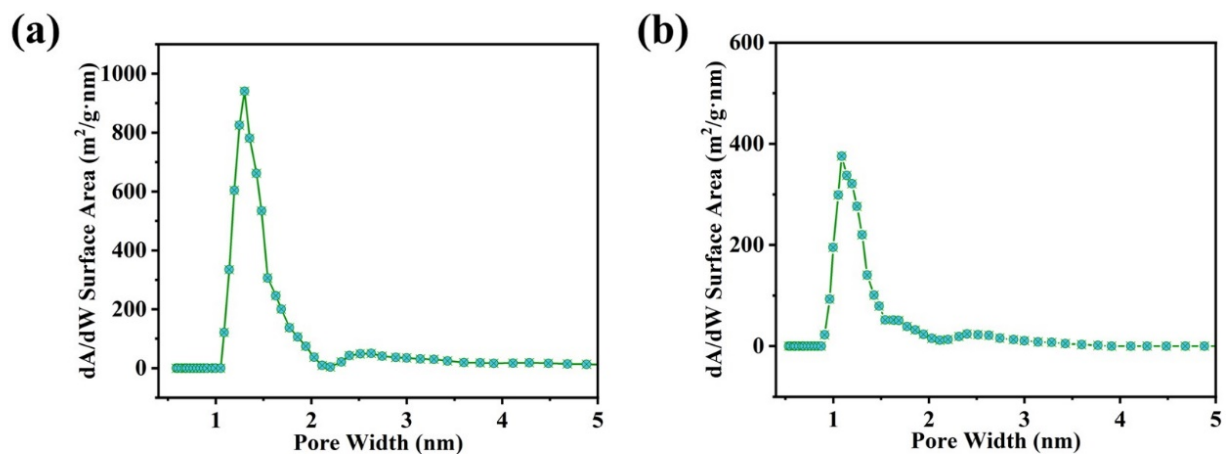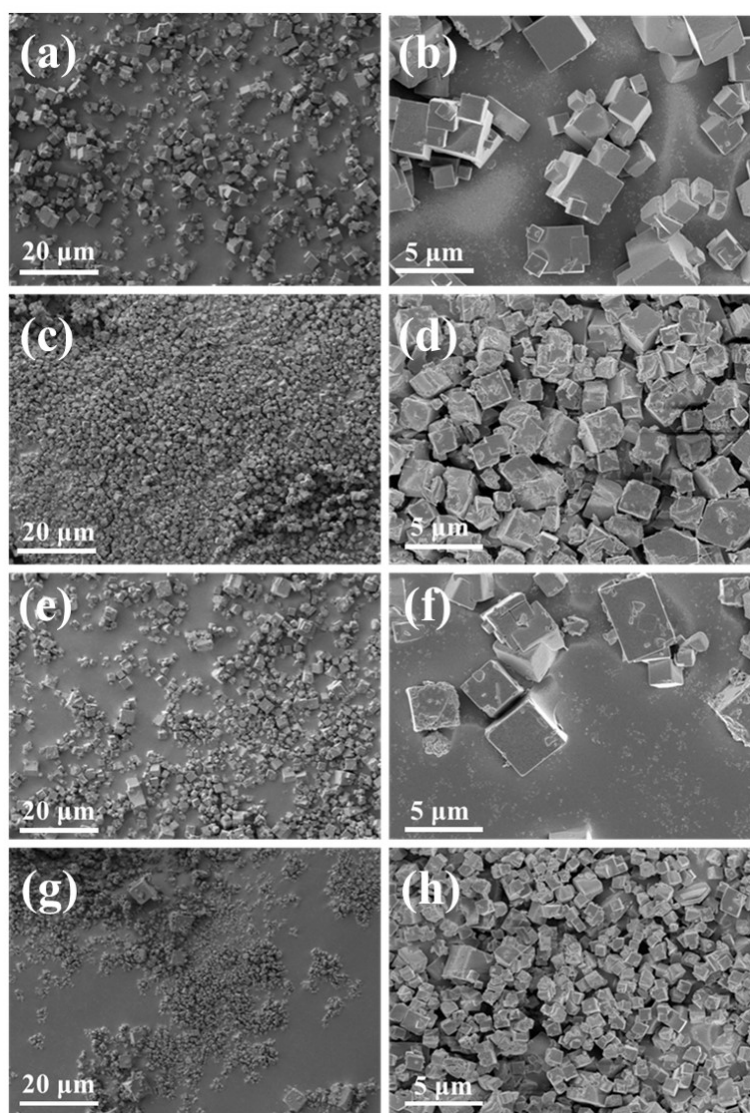
**Fig.S4** Pore size of ZrT-1(a) and ZrT-1-OH(b)



**Fig.S5** SEM images of ZrT-1 (a-d) and ZrT-1-OH (e-h) under a power of 75 W: (a,b) ZrT-1, 60 °C, 40kHz; (c,d) ZrT-1, 30 °C, 40kHz; (e,f) ZrT-1-OH, 60 °C, 40kHz; (g,h) ZrT-1-OH, 30 °C, 40kHz

**Fig.S6** Color change of TAR solution and Zr-MOCs before and after adsorption.

**Table.S1** Comparison of adsorption capacity for TAR between synthesized Zr-MOCs and reported materials.

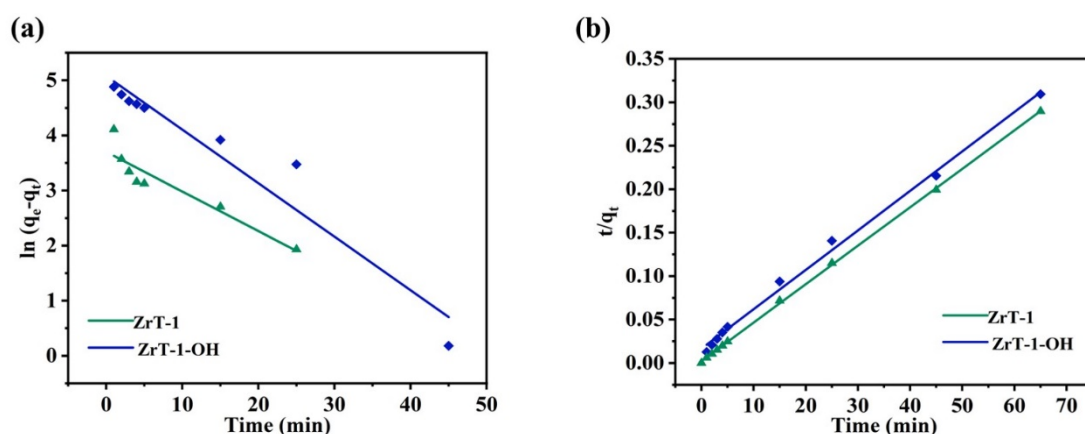| Adsorbent | $Q_{max}$ (mg/g) | $pH_{optimun}$ | C (mg/L) | T (°C) | $t_{eq}$ (min) | $S_{BET}$ ($m^2$/g) | Kinetic model | Isotherm model | Refs. |
|---|---|---|---|---|---|---|---|---|---|
| Porous chitosan sponge | 373.7 | 6.0 | 400 | 25 | 30 | 1150.0 | PSO and Elovich | - | 1 |
| Multi-walled carbon nanotubes | 85.09 | 3.0 | 50 | 25 | 60 | - | PSO | Langmuir | 2 |
| Activated red mud | 136.98 | 8.0 | 100 | 20 | 30 | - | PSO | Langmuir | 3 |
| Cu-DTO MOF | 309.2 | 2.0 | 25 | 50 | 30 | 119.6 | PSO | Freundlich | 4 |
| Chitosan-grafted Polyaniline | 584.0 | 7.2 | 400 | 25 | 120 | - | PSO | Freundlich | 5 |
| Double-layered hydroxide (ZnCl$_2$, AlCl$_3$) | 282.48 | 6.0 | 40 | 25 | 60 | - | PSO | Langmuir | 6 |
| Co$_3$O$_4$ nanoparticles | 204.3 | 4.0 | 100 | 40 | 90 | - | PSO | Freundlich | 7 |
| UiO-66@PVDF MOF beads | 77.51 | 2.0 | 40 | 50 | 120 | 360.74 | PSO | Langmuir | 8 |
| ZrT-1 | 238.6 | 3.0 | 50 | 25 | 65 | 424.2033 | PSO | Langmuir | This work |
| ZrT-1-OH | 225.3 | 3.0 | 50 | 25 | 65 | 853.7193 | PSO | Langmuir | This work |

**Fig.S7** Curves of pseudo-first-order (a) and pseudo-second-order (b) kinetics of TRA for Zr-MOCs.

**Table S2** The equilibrium capacities, pseudo-second-order rate constant, pseudo-second order rate constant and R2 values of Zr-MOCs for dyes adsorption.

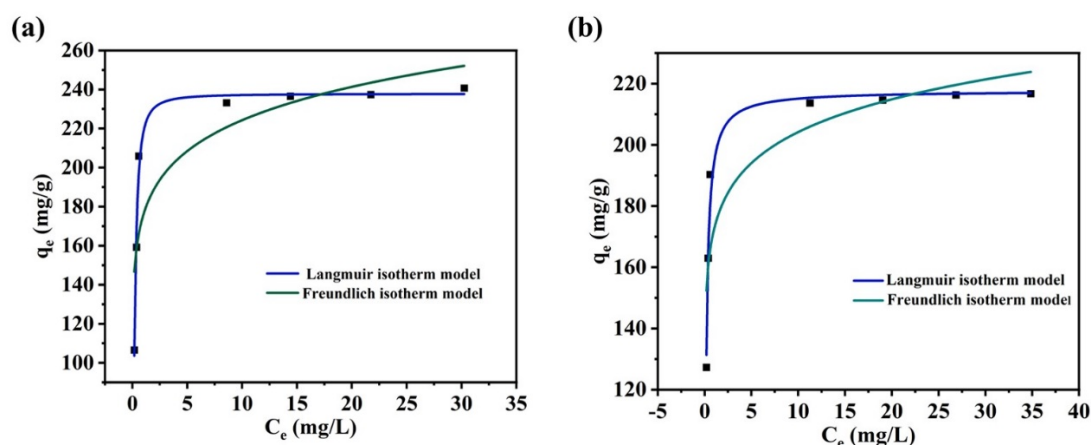| Adsorbent Dye | Pseudo-first-order | | | | Pseudo-second-order | | |
|---|---|---|---|---|---|---|---|
| | $q_{e\,(exp)}$(mg/g) | $K_1$ | $q_{e\,(cal)}$(mg/g) | $R^2$ | $K_2$ | $q_{e\,(cal)}$(mg/g) | $R^2$ |
| ZrT-1 | 224.31653 | -0.0719 | 40.45 | 0.868 | -0.00442 | 226.244 | 0.999 |
| ZrT-1-OH | 210.11212 | -0.0972 | 160.29 | 0.934 | -0.00454 | 220.26 | 0.996 |



**Fig.S8** ZrT-1 (a) and ZrT-1-OH (b) fitting by Langmuir isotherm model and Freundlich isotherm model.

**Table S3** Parameter values for different kinetic models

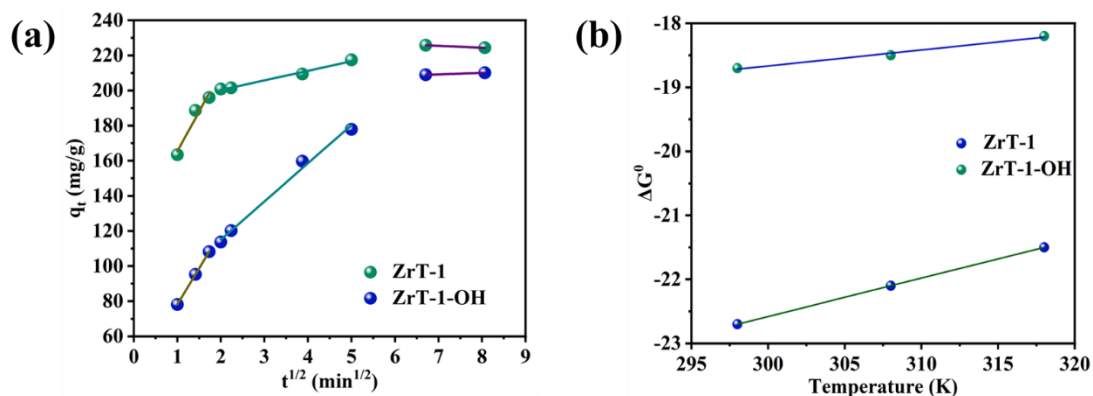| | Langmuir isothermal | | | Freundlich isothermal | | |
|---|---|---|---|---|---|---|
| | $K_L$ | $q_{max}$ | $R^2$ | $K_F$ | $1/n$ | $R^2$ |
| ZrT-1 | 5.44 | 241.9 | 0.96 | 175.85 | 0.1057 | 0.78 |
| ZrT-1-OH | 8.2 | 217.7 | 0.98 | 172.37 | 0.0736 | 0.82 |

**Fig.S9** Fitting by intra-particle diffusion kinetic models (a) and adsorption thermodynamic models (b).

**Table S4** Thermodynamic parameters for the adsorption of TAR using ZrT-1 and ZrT-1-OH.

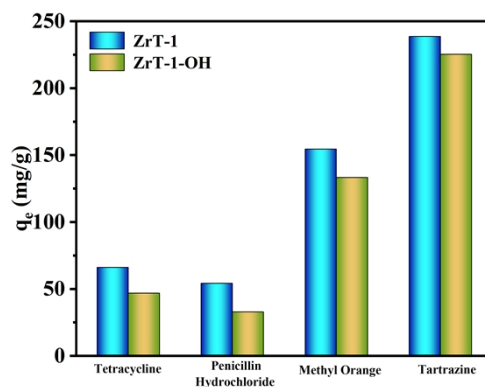| | $\triangle G$/ KJ mol$^{-1}$ | | | $\triangle H$/KJ mol$^{-1}$ | $\triangle S$/ KJ mol$^{-1}$k$^{-1}$ |
|---|---|---|---|---|---|
| | **298K** | **308K** | **318K** | | |
| ZrT-1 | -22.7 | -22.1 | -21.5 | -41.1 | -0.06 |
| ZrT-1-OH | -18.7 | -18.5 | -18.2 | -26.8 | -0.03 |



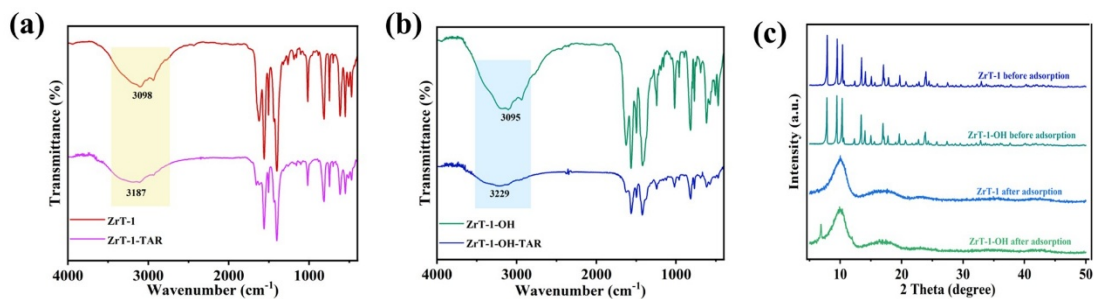Fig.S10 The adsorption capacity of Zr-MOCs for four pollutants.



**Fig.S11** FT-IR spectra of ZrT-1 (a) and ZrT-1-OH (b) before and after adsorption, along with XRD patterns (c) for comparison before and after adsorption.
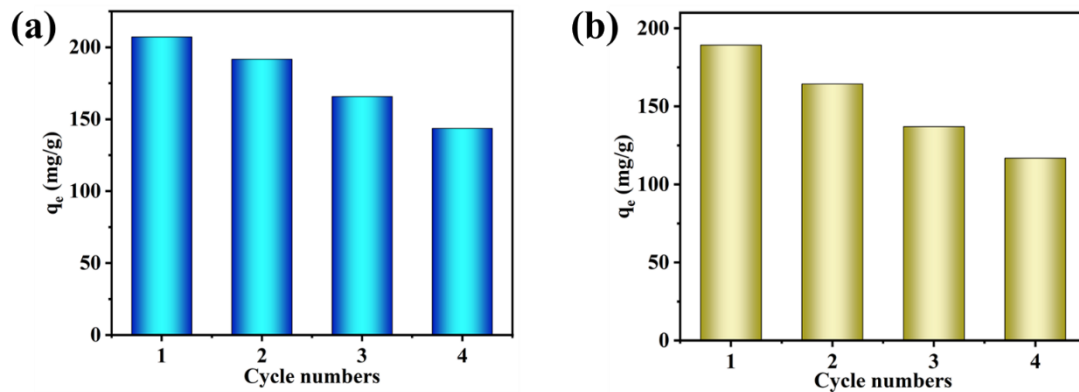
**Fig.S12** Adsorption capacity of ZrT-1 (a) and ZrT-1 (a) ZrT-1-OH (b) under different cycles.

# Reference

[S1]  V. M. Esquerdo, T. M. Quintana, G. L. Dotto and L. A. A. Pinto, *React. Kinet., Mech. Catal.*, 2015, **116**, 105–117.

[S2] J. Goscianska and R. Pietrzak, *Catal. Today*, 2015, **249**, 259–264.

[S3]  R. K. Gautam, S. Banerjee, M. A. Sanroman and M. C. Chattopadhyaya, *J. Environ. Chem. Eng.*, 2017, **5**, 328–340.

[S4]  I.-G. Bacioiu, L. Stoica, C. Constantin and A.-M. Stanescu, *Water, Air, Soil Pollut.*, 2017, **228**, 298.

[S5]  S. Sahnoun and M. Boutahala, *Int. J. Biol. Macromol.*, 2018, **114**, 1345–1353.

[S6]  H. Ouassif, E. M. Moujahid, R. Lahkale, R. Sadik, F. Z. Bouragba, E. M. Sabbar and M. Diouri, *Surf. Interfaces*, 2020, **18**, 100401.

[S7]  B. Zafar, S. S. Shafqat, M. N. Zafar, S. Haider, S. H. Sumrra, M. Zubair, N. Alwadai, F. H. Alshammari, A. S. Almuslem and M. S. Akhtar, *Mater. Today Commun.*, 2022, **33**, 104946.

[S8]  H. Singh, A. Goyal, S. K. Bhardwaj, M. Khatri and N. Bhardwaj, *Mater. Sci. Eng.: B*, 2023, **288**, 116165.